

Simulation of MPPT Algorithm Based Hybrid Wind-Solar-Fuel Cell Energy System

Kalpana. P¹, Venkata Pradeep. G²

^{1,2} Department of Electrical and Electronics Engineering, JNTU Anantapur

Abstract: This paper presents a new system configuration of the front-end rectifier stage for a hybrid wind/photovoltaic energy system. This configuration allows the two sources to supply the load separately or simultaneously depending on the availability of the energy sources. The inherent nature of this Cuk-SEPIC fused converter, additional input filters are not necessary to filter out high frequency harmonics. Harmonic content is detrimental for the generator lifespan, heating issues, and efficiency. The fused multiinput rectifier stage also allows Maximum Power Point Tracking (MPPT) to be used to extract maximum power from the wind and sun when it is available. An adaptive MPPT algorithm will be used for the wind system and a standard perturb and observe method will be used for the PV system. Operational analysis of the proposed system will be discussed in this paper. Simulation results are given to highlight the merits of the proposed circuit.

I. Introduction

When a source is unavailable or insufficient in meeting the load demands, the other energy source can compensate for the difference. Several hybrid wind/PV power systems with MPPT control have been proposed and discussed in works [1]- [5]. Most of the systems in literature use a separate DC/DC boost converter connected in parallel in the rectifier stage as shown in Figure 1 to perform the MPPT control for each the renewable energy power sources [1]-[4]. A simpler multiinput structure has been suggested by [5] that combine the sources from the DC-end while still achieving MPPT for each renewable source. The structure proposed by [5] is a fusion of the buck and buck-boost converter. The systems in literature require passive input filters to remove the high frequency current harmonics injected into wind turbine generators [6]. The harmonic content in the generator current decreases its lifespan and increases the power loss due to heating [6]. In this paper, an alternative multi-input rectifier structure is proposed for hybrid wind/solar energy systems. The proposed design is a fusion of the Cuk and SEPIC converters. The features of the proposed topology are: 1) the inherent nature of these two converters eliminates the need for separate input filters for PFC [7]-[8]; 2) it can support step up/down operations for each renewable source (can support wide ranges of PV and wind input); 3) MPPT can be realized for each source; 4) individual and simultaneous operation is supported.

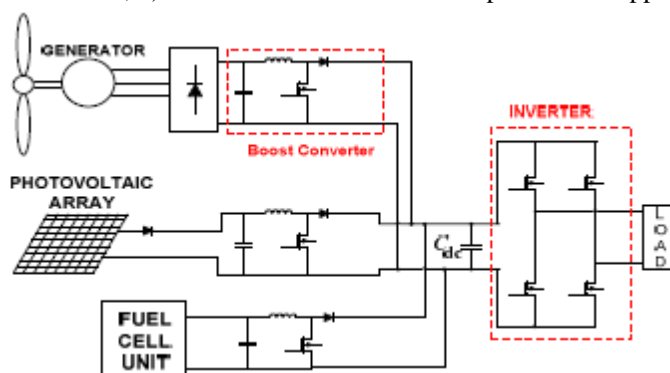


Figure 1: Hybrid system with multi-connected boost converter

II. Proposed Multi-Input Rectifier Stage

A system diagram of the proposed rectifier stage of a hybrid energy system is shown in Figure 2, where one of the inputs is connected to the output of the PV array and the other input connected to the output of a generator. The fusion of the two converters is achieved by reconfiguring the two existing diodes from each converter and the shared utilization of the Cuk output inductor by the SEPIC converter. This configuration

allows each converter to operate normally individually in the event that one source is unavailable. Figure 3 illustrates the case when only the wind source is available. In this case, $D1$ turns off and $D2$ turns on; the proposed circuit becomes a SEPIC converter and the input to output voltage relationship is given by (1). On the other hand, if only the P source is available, then $D2$ turns off and $D1$ will always be on and the circuit becomes a Cuk converter as shown in Figure 4. The input to output voltage relationship is given by (2). In both cases, both converters have step-up/down capability, which provide more design flexibility in the system if duty ratio control is utilized to perform MPPT control.

$$\frac{V_{dc}}{V_W} = \frac{d_2}{1-d_2} \quad (1)$$

$$\frac{V_{dc}}{V_{pv}} = \frac{d_1}{1-d_1} \quad (2)$$

Figure 5 illustrates the various switching states of the proposed converter. If the turn on duration of $M1$ is longer than $M2$, then the switching states will be state I, II, IV. Similarly, the switching states will be state I, III, IV if the switch conduction periods are vice versa. To provide a better explanation, the inductor current waveforms of each switching state are given as follows assuming that $d_2 > d_1$; hence only states I, III, IV are discussed in this example. In the following, $I_{i,PV}$ is the average input current from the PV source; $I_{i,W}$ is the RMS input current after the rectifier (wind case); and I_{dc} is the average system output current. The key waveforms that illustrate the switching states in this example are shown in Figure 6. The mathematical expression that relates the total output voltage and the two input sources will be illustrated in the next section.

State I (M1 on, M2 on):

$$i_{L1} = I_{i,PV} + \frac{V_{PV}}{L_1} t \quad 0 < t < d_1 T_s$$

$$i_{L2} = I_{dc} + \left(\frac{v_{c1} + v_{c2}}{L_2} \right) t \quad 0 < t < d_1 T_s$$

$$i_{L3} = I_{i,W} + \frac{V_W}{L_3} t \quad 0 < t < d_1 T_s$$

State III (M1 off, M2 on):

$$i_{L1} = I_{i,PV} + \left(\frac{V_{PV} - v_{c1}}{L_1} \right) t \quad d_1 T_s < t < d_2 T_s$$

$$i_{L2} = I_{dc} + \frac{v_{c2}}{L_2} t \quad d_1 T_s < t < d_2 T_s$$

$$i_{L3} = I_{i,W} + \frac{V_W}{L_3} t \quad d_1 T_s < t < d_2 T_s$$

State IV (M1 off, M2 off):

$$i_{L1} = I_{i,PV} + \left(\frac{V_{PV} - v_{c1}}{L_1} \right) t \quad d_2 T_s < t < T_s$$

$$i_{L2} = I_{dc} - \frac{V_{dc}}{L_2} t \quad d_2 T_s < t < T_s$$

$$i_{L3} = I_{i,W} + \left(\frac{V_W - v_{c2} - V_{dc}}{L_3} \right) t \quad d_2 T_s < t < T_s$$

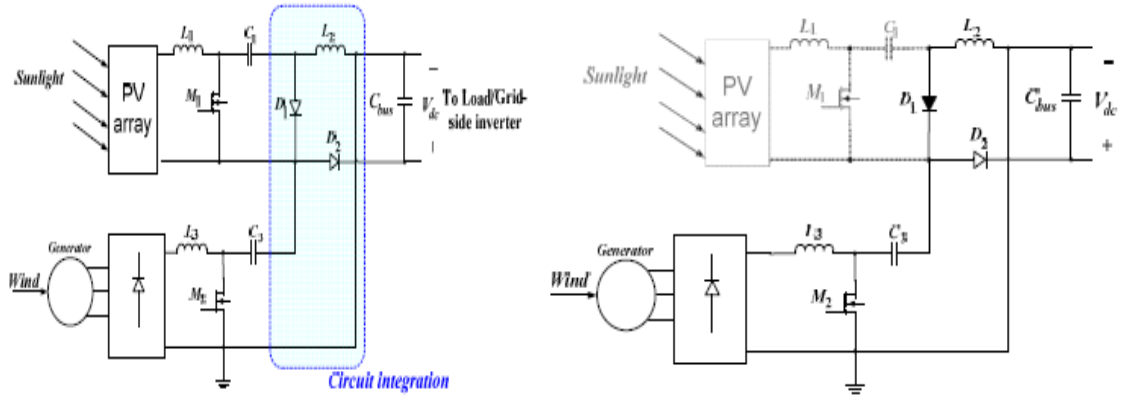


Figure 2: Proposed rectifier stage for a Hybrid wind/PV system, Figure 3: Only wind source is operational (SEPIC)

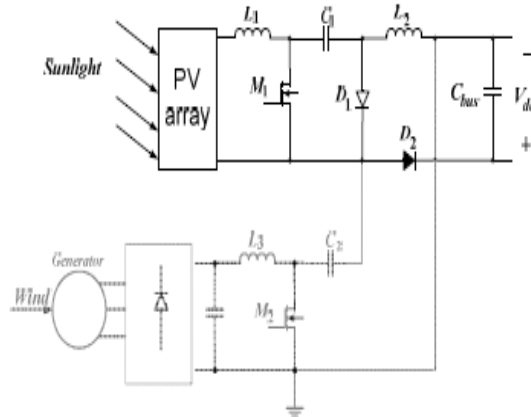


Figure 4: Only PV source is operation (Cuk)

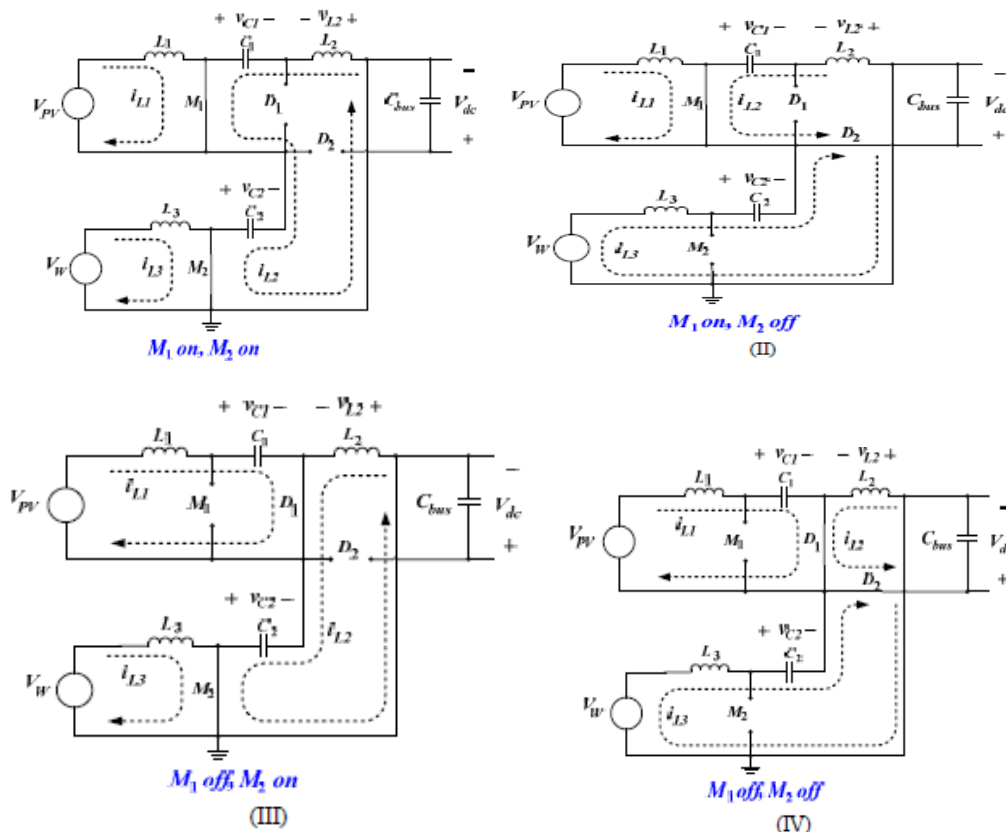


Figure 5 (I-IV): switching states within a switching cycle

III. Analysis Of Proposed Circuit

To find an expression for the output DC bus voltage, V_{dc} , the volt-balance of the output inductor, L_2 , is examined according to Figure 6 with $d_2 > d_1$. Since the net change in the voltage of L_2 is zero, applying volt-balance to L_2 results in (3). The expression that relates the average output DC voltage (V_{dc}) to the capacitor voltages (v_{c1} and v_{c2}) is then obtained as shown in (4), where v_{c1} and v_{c2} can then be obtained by applying volt-balance to L_1 and L_3 [9]. The final expression that relates the average output voltage and the two input sources (V_W and V_{PV}) is then given by (5). It is observed that V_{dc} is simply the sum of the two output voltages of the Cuk and SEPIC converter. This further implies that V_{dc} can be controlled by d_1 and d_2 individually or simultaneously.

$$(v_{c1} + v_{c2})d_1T_s + (V_{c2})(d_2 - d_1)T_s + (1 - d_2)(-v_{dc})T_s = 0 \quad (3)$$

$$v_{dc} = \left(\frac{d_1}{1-d_2}\right)v_{c1} + \left(\frac{d_2}{1-d_2}\right)v_{c2} \quad (4)$$

$$v_{dc} = \left(\frac{d_1}{1-d_1}\right)v_{pv} + \left(\frac{d_2}{1-d_2}\right)v_w \quad (5)$$

The switches voltage and current characteristics are also provided in this section. The voltage stress is given by (6) and (7) respectively. As for the current stress, it is observed from Figure 6 that the peak current always occurs at the end of the on-time of the MOSFET. Both the Cuk and SEPIC MOSFET current consists of both the input current and the capacitors (C_1 or C_2) current. The peak current stress of M_1 and M_2 are given by (8) and (10) respectively. L_{eq1} and L_{eq2} , given by (9) and (11), represent the equivalent inductance of Cuk and SEPIC converter respectively. The PV output current, which is also equal to the average input current of the Cuk converter is given in (12). It can be observed that the average inductor current is a function of its respective duty cycle (d_1). Therefore by adjusting the respective duty cycles for each energy source, maximum power point tracking can be achieved.

$$V_{ds1} = V_{pv} \left(1 + \frac{d_1}{1-d_1}\right) \quad (6)$$

$$V_{ds2} = V_w \left(1 + \frac{d_2}{1-d_2}\right) \quad (7)$$

$$i_{ds1,pk} = I_{i,pv} + I_{dc,avg} + \frac{V_{pv}d_1T_s}{2L_{eq1}} \quad (8)$$

$$L_{eq1} = \frac{L_1L_2}{L_1+L_2} \quad (9)$$

$$i_{ds2,pk} = I_{i,pv} + I_{dc,avg} + \frac{V_{pv}d_2T_s}{2L_{eq1}} \quad (10)$$

$$L_{eq2} = \frac{L_3L_2}{L_3+L_2} \quad (11)$$

$$I_{i,pv} = \frac{P_0}{V_{dc}} \frac{d_1}{1-d_1} \quad (12)$$

IV. Mppt Control Of Proposed Circuit

A common inherent drawback of wind and PV systems is the intermittent nature of their energy sources. Wind energy is capable of supplying large amounts of power but its presence is highly unpredictable as it can be here one moment and gone in another. Solar energy is present throughout the day, but the solar irradiation levels vary due to sun intensity and unpredictable shadows cast by clouds, birds, trees, etc. These drawbacks tend to make these renewable systems inefficient. However, by incorporating maximum power point tracking (MPPT) algorithms, the systems' power transfer efficiency can be improved significantly. To describe a wind turbine's power characteristic, equation (13) describes the mechanical power that is generated by the wind.

$$p_m = 0.5\rho AC_p(\lambda, \beta)v_w^3$$

Where

P=air density,

A=rotor swept area,

$c_p(\lambda, \beta)$ = power coefficient function,

λ =tip speed ratio,

β =pitch angle,

v_w = wind speed

The power coefficient (C_p) is a nonlinear function that represents the efficiency of the wind turbine to convert wind energy into mechanical energy. It is dependent on two variables, the tip speed ratio (TSR) and the pitch angle. The TSR, λ , refers to a ratio of the turbine angular speed over the wind speed. The mathematical representation of the TSR is given by (14) [10]. The pitch angle, β , refers to the angle in which the turbine blades are aligned with respect to its longitudinal axis.

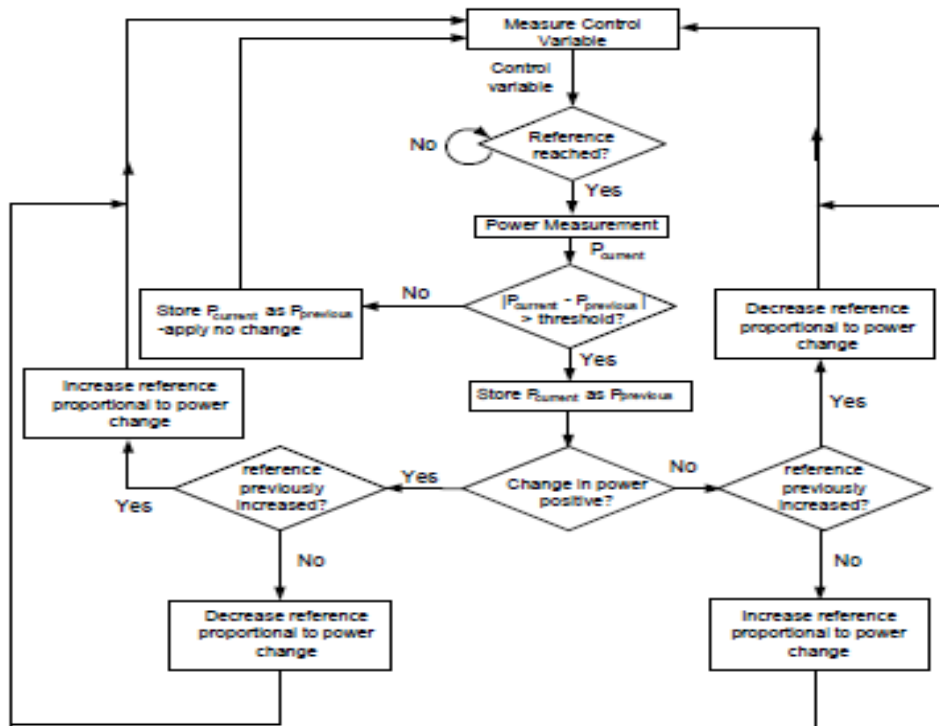


Figure 6: General MPPT Flow Chart for wind and PV

V. Simulation Results

In this section, simulation results from MATLAB 7.8 is given to verify that proposed multi-input rectifier stage can support individual as well as simultaneous operation. The specifications for the design example are given in TABLE I. Figure 10 illustrates the system under the condition where the wind source has failed and only the PV source (Cuk converter mode) is supplying power to the load. Figure 11 illustrates the system where only the wind turbine generates power to the load (SEPIC converter mode). Finally, Figure 12 illustrates the simultaneous operation (Cuk-SEPIC fusion mode) of the two sources where M2 has a longer conduction cycle (converter states I, IV and III—see Figure 5).

TABLE I. Design Specifications

Output power(W)	3Kw
Output voltage	500V
Switching frequency	20kHz

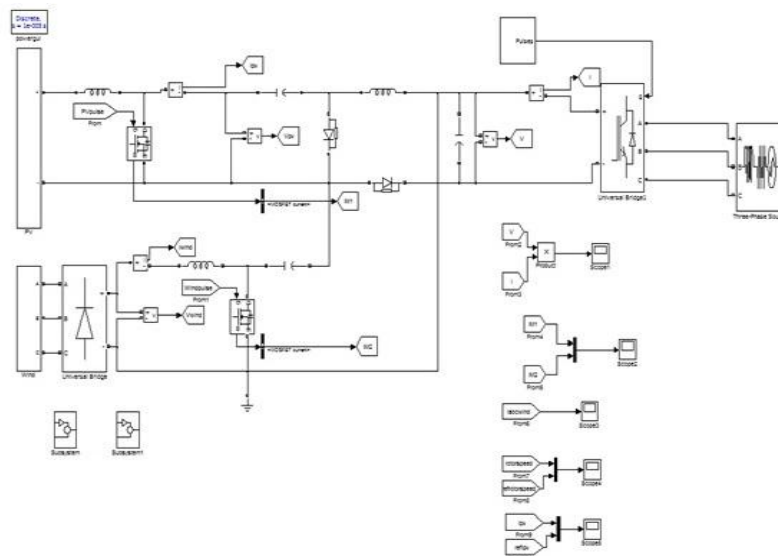


Fig 7: Hybrid solar wind

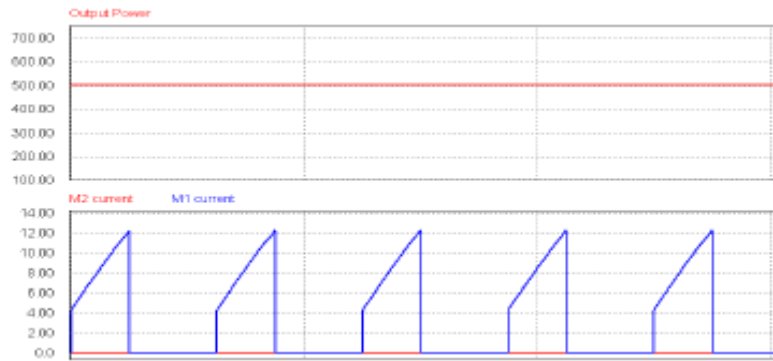


Figure 8 : Individual operation with only PV source (Cuk operation) Top: Output power, Bottom: Switch currents (M1 and M2)

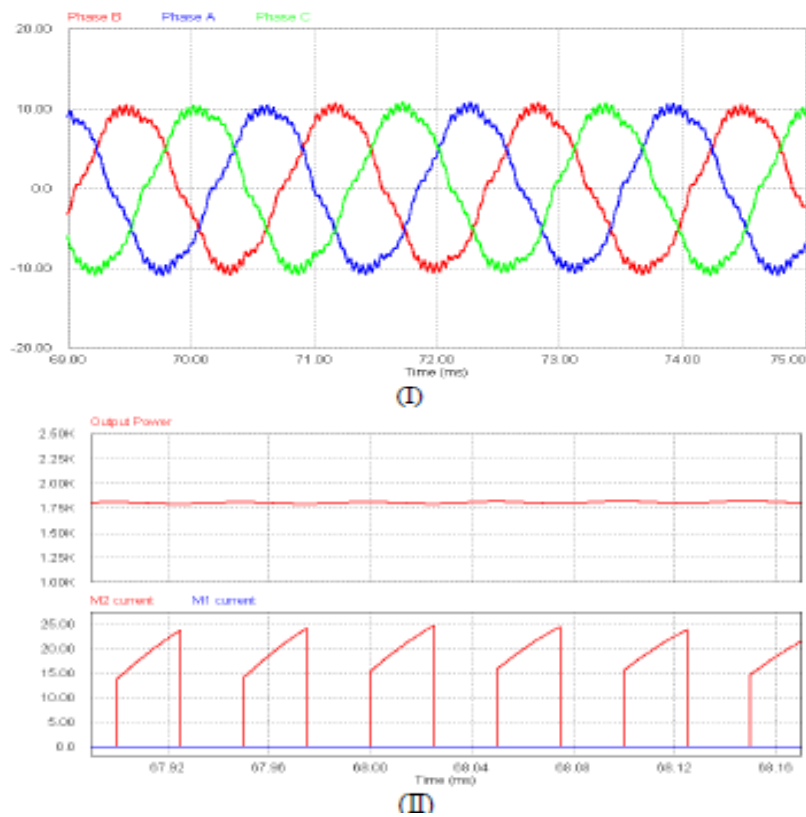
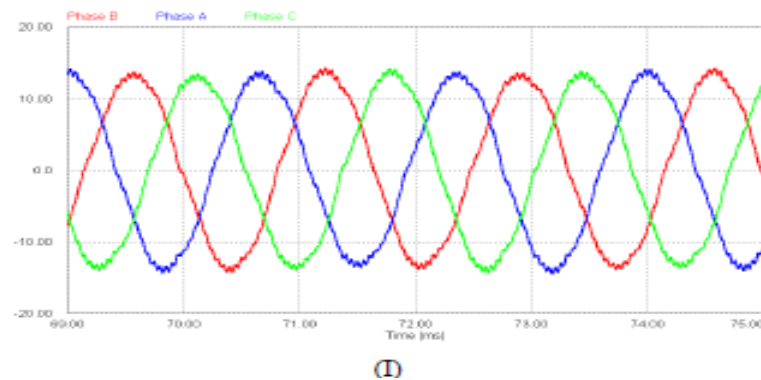


Figure 9 : Individual operation with only wind source (SEPIC operation) (I) The injected three phase generator current; (II) Top: Output power, Bottom: Switch currents (M1 and M2)



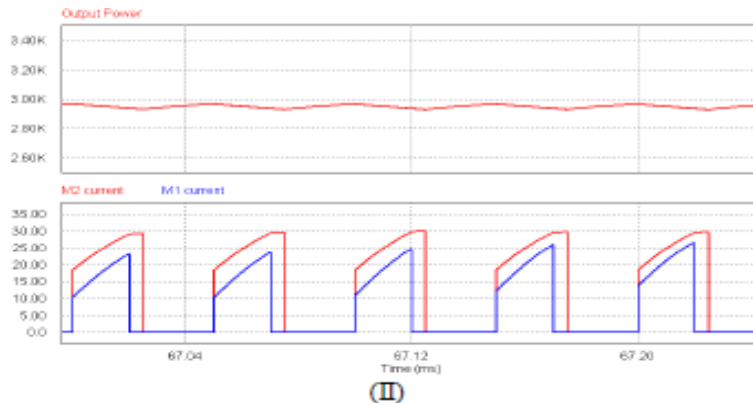


Figure 10 : Simultaneous operation with both wind and PV source (Fusion mode with Cuk and SEPIC)(I) The injected three phase generator current; (II) Top: Output power, Bottom: Switch currents (M1 and M2)

Figure 11 and 12 illustrates the MPPT operation of the PV component of the system (Cuk operation) and the Wind component of the system (SEPIC operation) respectively.

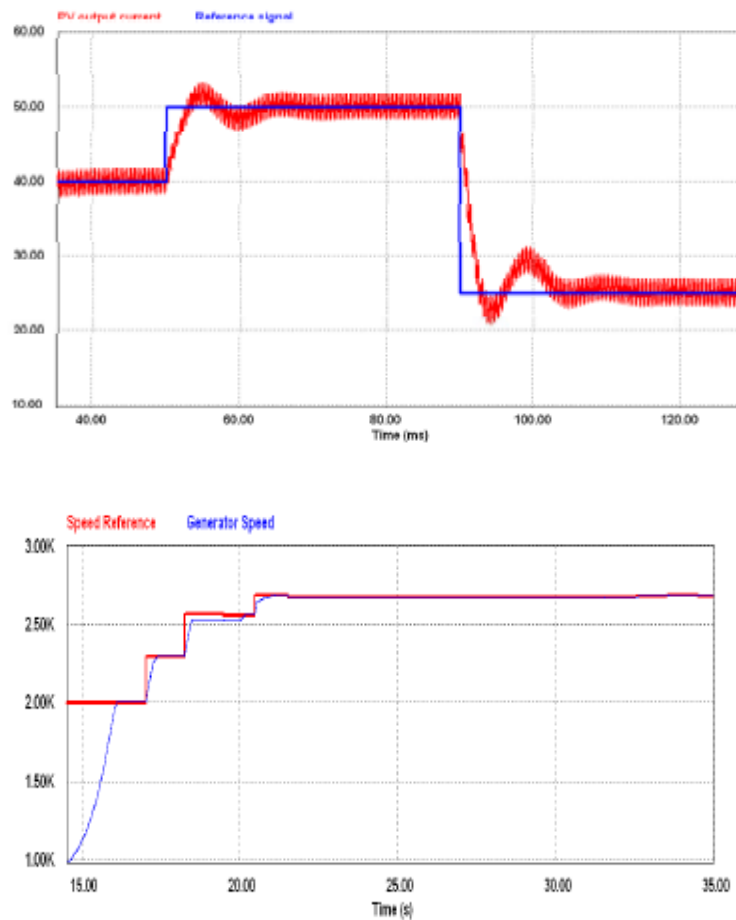


Figure 11 : Solar MPPT – PV output current and reference current signal (Cuk operation) and Figure 12 : Wind MPPT – Generator speed and reference speed signal (SEPIC operation)

VI. Conclusion

In this paper a new multi-input Cuk-SEPIC rectifier stage for hybrid wind/solar energy systems has been presented. The features of this circuit are: 1) additional input filters are not necessary to filter out high frequency harmonics; 2) both renewable sources can be stepped up/down (supports wide ranges of PV and wind input); 3) MPPT can be realized for each source; 4) individual and simultaneous operation is supported. Simulation results have been presented to verify the features of the proposed topology.

REFERENCES

- [1] S.K. Kim, J.H. Jeon, C.H. Cho, J.B. Ahn, and S.H. Kwon, "Dynamic Modeling and Control of a Grid-Connected Hybrid Generation System with Versatile Power Transfer," *IEEE Transactions on Industrial Electronics*, vol. 55, pp. 1677-1688, April 2008.
- [2] D. Das, R. Esmaili, L. Xu, D. Nichols, "An Optimal Design of a Grid Connected Hybrid Wind/Photovoltaic/Fuel Cell System for Distributed Energy Production," in *Proc. IEEE Industrial Electronics Conference*, pp. 2499-2504, Nov. 2005.
- [3] N. A. Ahmed, M. Miyatake, and A. K. Al-Othman, "Power fluctuations suppression of stand-alone hybrid generation combining solar photovoltaic/wind turbine and fuel cell systems," in *Proc. Of Energy Conversion and Management*, Vol. 49, pp. 2711-2719, October 2008.
- [4] S. Jain, and V. Agarwal, "An Integrated Hybrid Power Supply for Distributed Generation Applications Fed by Nonconventional Energy Sources," *IEEE Transactions on Energy Conversion*, vol. 23, June
- [5] Y.M. Chen, Y.C. Liu, S.C. Hung, and C.S. Cheng, "Multi-Input Inverter for Grid-Connected Hybrid PV/Wind Power System," *IEEE Transactions on Power Electronics*, vol. 22, May 2007.
- [6] dos Reis, F.S., Tan, K. and Islam, S., "Using PFC for harmonic mitigation in wind turbine energy conversion systems" in *Proc. of the IECON 2004 Conference*, pp. 3100- 3105, Nov. 2004
- [7] R. W. Erickson, "Some Topologies of High Quality Rectifiers" in the *Proc. of the First International Conference on Energy, Power, and Motion Control*, May 1997.
- [8] D. S. L. Simonetti, J. Sebasti'an, and J. Uceda, "The Discontinuous Conduction Mode Sepic and Cuk Power Factor Preregulators: Analysis and Design" *IEEE Trans. On Industrial Electronics*, vol. 44, no. 5, 1997
- [9] N. Mohan, T. Undeland, and W. Robbins, "Power Electronics: Converters, Applications, and Design," John Wiley & Sons, Inc., 2003.
- [10] J. Marques, H. Pinheiro, H. Grundling, J. Pinheiro, and H. Hey, "A Survey on Variable-Speed Wind Turbine System," *Proceedings of Brazilian Conference of Electronics of Power*, vol. 1, pp. 732-738, 2003.
- [11] F. Lassier and T. G. Ang, "Photovoltaic Engineering Handbook" 1990
- [12] Global Wind Energy Council (GWEC), "Global wind 2008 report," June 2009.
- [13] L. Pang, H. Wang, Y. Li, J. Wang, and Z. Wang, "Analysis of Photovoltaic Charging System Based on MPPT," *Proceedings of Pacific-Asia Workshop on Computational Intelligence and Industrial Application 2008 (PACIIA '08)*, Dec 2008, pp. 498-501.